Birefringence arising from the reorientation of the polarizability anisotropy of molecules in collisionless gases

C. H. Lin*
Ames Research Center, NASA, Moffett Field, California 94035

J. P. Heritage† and T. K. Gustafson†
Department of Electrical Engineering and Computer Sciences and the Electronic Research Laboratory, University of California, Berkeley, California 94720

R. Y. Chiao
Department of Physics, University of California, Berkeley, California 94720

J. P. McTague‡
Department of Chemistry, University of California, Los Angeles, California 90024
(Received 28 January 1974; revised manuscript received 11 August 1975)

The refractive-index change in a collisionless gas is evaluated from the Stark shifts of the rotational energy levels that arise from the polarizability anisotropy. In the limit of an extremely-short-duration excitation, a multilevel coherent effect results in delayed refractive-index bursts. Both stationary and transient responses of this birefringence to an optical field are considered for symmetric-top molecules, with particular emphasis on the special case of linear molecules.

I. INTRODUCTION

The birefringence induced by a uniform electromagnetic field in a fluid composed of anisotropic molecules arises primarily from the reorientation of the molecules due to their interaction with the field through the molecular electric dipole moment[1] and the anisotropy of the static polarizability.[2] The present work is restricted to the rotational response of polar and nonpolar molecules excited by short optical pulses for which the interaction is primarily through the polarizability anisotropy. Though the permanent dipole interaction dominates for frequencies of the applied field ranging from dc to microwave, at higher frequencies it plays a diminishing role. In liquids, this rolloff of the rotational response with increasing frequency results from a damping of the rotational motion due to viscous interaction with neighboring molecules. For gases, collisional or inertial effects are responsible for such a rolloff. Consequently, for both liquids and gases, at optical frequencies the interaction through the permanent dipole moment is extremely weak.

Molecular reorientation resulting from the interaction through the polarizability anisotropy depends on the square of the electric field, so that even for optical frequencies there are low-frequency components that produce a significant rotational response,[2] and hence induced birefringence. This nonlinear optical birefringence has been treated for liquids by a generalization of Debye's classical theory of molecular rotation.[1,3] The result shows that the angular distribution of the molecules achieves thermodynamic equilibrium in a characteristic time that is one-third the viscous relaxation time deduced by Debye for polar molecules. This characteristic time, typically of the order of tens of picoseconds, is much larger than the mean time between molecular collisions (collision time).

In gases for which the collision time is much greater than the rotational period of the molecules, quantization of the rotational motion is important. Nevertheless, when the gas interacts with a smooth light pulse having a duration much longer than the collision time, thermodynamic equilibrium is maintained just as in liquids. For this case, the classical thermodynamic approach employed by Bloembergen and Lallemand[3] is a good approximation.

The primary concern of this paper is in the nonequilibrium situation, i.e., birefringence in gases induced by optical disturbances shorter than the collision time. The gas is thus considered to be "collisionless," and the momentum associated with the molecular rotation must be considered explicitly.

We first deduce a nonequilibrium-induced refractive-index change for linear molecules from the quartic and higher-order Stark shifts of the rotational energy levels evaluated from time-independent perturbation theory. Such an approach is strictly valid for an interaction with optical pulses which, although less than the collision time in duration, are longer than the inverse of the fund-

amental rotational transition frequency. However, even for a much shorter excitation, the transient response of the gas during the excitation is in many cases of experimental interest quite well approximated by this stationary theory. The lowest-order nonlinear refractive-index change which is directly proportional to the square of the electric field intensity is tabulated for several gases composed of linear molecules or symmetric-top molecules. These range from 4×10^{-13} (statvolt/cm)$^{-2}$ (mole/cm^3)$^{-1}$ for H_2 at 35 °K to 2×10^{-10} (statvolt/cm)$^{-2}$(mole/cm^3)$^{-1}$ for CS_2 at 320 °K. Analytic expressions for the refractive-index change in both the high-temperature limit and the low-temperature limit are given. Saturation of this refractive-index change for high-field intensity is also discussed.

When the optical pulses are shorter than both the collision time and the inverse of the fundamental quadrupole transition frequency, the molecular rotational response cannot follow the excitation instantaneously. Hence, the refractive-index change has an explicit time dependence and can persist subsequent to excitation. For such an ultrashort excitation, the refractive-index change is deduced from the density matrix equations for the molecular rotation. For a gas composed of linear molecules, it has already been shown[4] that after excitation with a single light pulse a periodic recurrence of the birefringence should result. These recurrences, which are due to quantum interference, can have an extremely short duration since many rotational levels can contribute. The individual echoic bursts should be separated by a time given by $1/4Bc$, where B is the rotational constant of the molecules in wave numbers and eventually should decay away due to collisional and Doppler effects.

In the present paper, this explicitly time-dependent refractive-index change has been investigated more extensively. In particular, we consider the transient refractive-index change during the presence of the optical excitation which in many situations is approximated well by the stationary results. The influence of the excitation-pulse width, the molecular rotational constant, and the gas temperature on the amplitude and the duration of the refractive-index bursts is also considered in detail. In addition, the results are generalized to include symmetric-top molecules.

The paper is divided into seven sections. In Sec. II, the Hamiltonian describing the interaction between molecules possessing a linear but anisotropic polarizability and an optical field is considered. In Sec. III the time-dependent perturbation calculation of the quartic and higher-order Stark shifts of the rotational energy levels of linear molecules is given and the induced refractive-index change for a gas composed of such molecules is determined. In Sec. IV a general expression for the lowest-order time-dependent nonlinear refractive-index change for gases composed of symmetric-top molecules is derived from the density-matrix representation of the rotational states. In Sec. V, we determine the stationary refractive-index change for symmetric-top molecules as a limit of the time-dependent expression obtained in Sec. IV and compare this result with that for a linear molecular gas. In Sec. VI, the time-dependent behavior of symmetric-top molecules is investigated and the special case of linear molecules is discussed in detail. In Sec. VII, the possibility of detecting the echoic refractive-index bursts, its application, and integral properties of the time-dependent refractive-index change are discussed.

II. PERTURBATION HAMILTONIAN FOR LINEAR POLARIZABLE MOLECULES

In this section, we define the Hamiltonian that describes the interaction between the rotational energy levels of linear molecules with an electric field oscillating at optical frequencies. The interaction is assumed to arise through the anisotropic polarizability and the optical intensity which is, in general, time-varying.

Linear molecules are particularly easy to treat since the polarizability is characterized by only two components: $\alpha_\parallel$, the polarizability along the molecular axis, and $\alpha_\perp$, that perpendicular to the molecular axis. The change in the potential energy of the rotational states produced by the interaction of the molecules with the radiation field is a function of $\Delta\alpha = \alpha_\parallel - \alpha_\perp$, the anisotropy, and θ, the angle between the molecular symmetry axis and some fixed direction in space. The latter is chosen to be the direction of the component of the angular momentum which commutes with the square of the magnitude of the total-angular-momentum vector.

For a linearly polarized optical field propagating in the z direction, the electric field is written in the form:

$$\vec{E} = [\tfrac{1}{2}E_0(t,z)e^{i(\omega t - kz)} + \text{c.c.}]\hat{a}_x , \tag{1}$$

where $\hat{a}_x$ is a unit vector specifying the polarization direction of the field and c.c. represents the complex conjugate of the first term. In this case, $\hat{a}_x$ is chosen as the projection axis for the commuting component of the angular momentum vector. $E_0(t,z)$, the electric field amplitude, is assumed to vary slowly in time ($\partial E_0/\partial t \ll \omega$) and in space ($\partial E_0/\partial z \ll k$). In all cases, the reaction of

the medium on the field is neglected. Consequently, $E_0(t,z) \simeq E_0[t-(k/\omega)z]$, where the propagation constant k is equal to ω/c, c being the speed of light in the gas.

The perturbing Hamiltonian for such a linearly polarized field is

$$H' = -\tfrac{1}{2}\Delta\alpha\langle\vec{E}\cdot\vec{E}\rangle\cos^2\theta - \tfrac{1}{2}\alpha_\perp\langle\vec{E}\cdot\vec{E}\rangle, \qquad (2)$$

in which $\langle\vec{E}\cdot\vec{E}\rangle$ is the average over an optical cycle of the square of the electric field amplitude, or $E_0(t,z)E_0^*(t,z)/2$. Such an average results since only the low-frequency term proportional to the time-averaged intensity of the electric field can appreciably perturb the molecular rotational energy states. The angular response of the molecules to the torque at frequency 2ω of $\langle\vec{E}\cdot\vec{E}\rangle$ is extremely weak because of molecular inertia.

If the optical pulse is circularly polarized and propagating in the z direction, the plane containing the electric field vector is defined by the mutually orthogonal unit vectors $\hat{a}_x$ and $\hat{a}_y$. The electric field vector can be written in the form

$$\vec{E} = [E_0(t,z)/2\sqrt{2}]\,[e^{i(\omega t-kz)}(\hat{a}_x + i\hat{a}_y) + \text{c.c.}]. \qquad (3)$$

For this polarization, the direction of propagation $\hat{a}_z$ is also chosen as the direction of the commuting component of the angular momentum. The perturbation Hamiltonian for this case is

$$H' = -\tfrac{1}{4}\Delta\alpha\langle\vec{E}\cdot\vec{E}\rangle\sin^2\theta - \tfrac{1}{2}\alpha_\perp\langle\vec{E}\cdot\vec{E}\rangle\,. \qquad (4)$$

III. STATIONARY REFRACTIVE-INDEX CHANGE FOR GASES COMPOSED OF LINEAR MOLECULES

In many of the experiments anticipated, the intensity of the optical excitation is expected to vary negligibly for times much shorter than the period determined by the transitions between the most highly populated rotational levels of the molecule. The refractive-index change induced during excitation with the optical pulse is then dependent primarily on the electric field intensity and not explicitly on time. A stationary solution of the Schrödinger equation is quite adequate for this portion of the response. This considerably simplifies the calculation and allows a simple estimate of the refractive-index response for particular molecular gases. The influence of saturation due to a high laser-field intensity is also more easily treated in the absence of an explicit time dependence.

The intensity dependent optical index of refraction,

$$n = n_0 + n_2\langle\vec{E}\cdot\vec{E}\rangle + n_4\langle\vec{E}\cdot\vec{E}\rangle^2 + n^6\langle\vec{E}\cdot\vec{E}\rangle^3,$$

can be obtained from the energy change ΔW induced by the presence of the electric field. Since

$$-4\pi N\frac{\partial\Delta W}{\partial E_0^*}\frac{1}{E_0} = -8\pi N\frac{\partial\Delta W}{\partial\langle\vec{E}\cdot\vec{E}\rangle}$$

is the susceptibility, where N is the number density,

$$n = \left(1 - 8\pi N\frac{\partial\Delta W}{\partial\langle\vec{E}\cdot\vec{E}\rangle}\right)^{1/2}$$

$$\simeq n_0 + \left(1 - n_0^2 - 8\pi N\frac{\partial\Delta W}{\partial\langle\vec{E}\cdot\vec{E}\rangle}\right)\Big/ 2n_0 \qquad (5)$$

assuming a dilute gas. The energy change ΔW is obtained from the Stark shifts of the rotational energy levels of the molecules.

There are two limiting situations which should be distinguished. The first occurs for optical pulses much longer than the collision time. The presence of collisions assures that the population distribution of the Stark-shifted energy levels is the thermodynamic equilibrium case as labeled by Boltzmann. In Appendix B, it is shown that both the quadratic and the quartic Stark shifts contribute to the coefficient n_2, which to a good approximation is given by the usual classical expression[3]:

$$(4\pi N/45)(\Delta\alpha)^2/kTn_0.$$

The second case is based on an absence of molecular collisions and thus is valid for optical pulses much shorter than the mean collision time. For this case, which is the primary concern of the present paper, the population of each shifted rotational level is frozen to the value determined by the initial zero-field Boltzmann distribution. The total energy change due to the Stark shifts is then

$$\Delta W = \frac{1}{Z}\sum_{J=0}^{\infty}\sum_{M=-J}^{+J} E_{J,M}\exp(-E_{J,M}^{(0)}/kT), \qquad (6)$$

where $E_{J,M}^{(0)}$ is the unperturbed rotational energy eigenvalue corresponding to a particular angular quantum number J and its projection M along the chosen fixed axis. Z is the partition function,

$$Z = \sum_{J=0}^{\infty}(2J+1)\exp(-E_{J,M}^{(0)}/kT);$$

$E_{J,M}$ is the perturbed rotational energy eigenvalue corresponding to the unperturbed Hamiltonian plus the interaction Hamiltonian of Eq. (2) or (4).

The appropriate solutions of the time-independent Schrödinger equation for the Hamiltonian of Eq. (2) or (4) are the spheroidal wave functions.[5] Cal-

culation of the corresponding perturbed rotational energy eigenvalue $E_{J,M}$ presents severe difficulties and has not been expressed analytically for an arbitrary field strength. The usual perturbation expansion, which is useful when the electric field is weak, is expressed as

$$E_{J,M}=hBc(\lambda_0+K\lambda_1+K^2\lambda_2+\cdots)-\tfrac{1}{2}\alpha_1\langle\vec{E}\cdot\vec{E}\rangle, \tag{7}$$

with K the perturbation expansion parameter, $\frac{1}{2}\Delta\alpha\langle\vec{E}\cdot\vec{E}\rangle/hBc$, and $\lambda_0 hBc$ is the unperturbed energy eigenvalue $J(J+1)hBc$. Values for $\lambda_1, \lambda_2, \lambda_3, \ldots$, in terms of increasing numbers of algebraic terms, as obtained from the standard perturbation approach are tabulated in Ref. 5. These can only be used as a starting point for the refractive-index calculation. Considerable effort is involved in combining the factors and in simplifying the resultant expressions.

If Eq. (7) is substituted into Eq. (6), ΔW for the collisionless case can be expressed as

$$\langle\Delta W\rangle=hBc\eta\sum_i N_i(\eta)K^i/Z\eta, \tag{8}$$

where the sums

$$N_i(\eta)=\sum_{J=0}^{\infty}\sum_{M=-J}^{J}\lambda_i e^{-J(J+1)\eta} \quad \text{and} \quad \eta=\frac{hBc}{kT}.$$

The first three coefficients in the nonlinear refractive-index expression, obtained from Eqs. (8) and (6) are

$$n_2=-\frac{2\pi N}{kTn_0}N_2(\eta)\frac{\Delta\alpha^2}{Z\eta}, \tag{9a}$$

$$n_4=\frac{3\pi N}{2kThBcn_0}N_3(\eta)\frac{\Delta\alpha^3}{Z\eta}, \tag{9b}$$

$$n_6=\frac{\pi N}{kT(hBc)^2n_0}N_4(\eta)\frac{\Delta\alpha^4}{Z\eta}. \tag{9c}$$

Considerable simplification occurs if sum rules over the projection quantum number M for the coefficients λ_i of the various orders in the perturbation expansion can be obtained. We thus wish to consider the pertinent aspects of the perturbation theory more deeply and in particular to outline the calculation of these.

For this, the collisionless case, the nonlinear refractive-index change is independent of the quadratic Stark shift $hBC\lambda_1 K$. However, as pointed out earlier and in Appendix B, this can contribute to the coefficient n_2 after collisions have significantly thermalized the population among the perturbed states.

For both linear and circular polarization the quadratic shifts, which respectively are [6,7]

$$\Delta W_1=K\lambda_1 hBc=-\tfrac{1}{2}\Delta\alpha\langle\vec{E}\cdot\vec{E}\rangle\frac{2J(J+1)-2M^2-1}{(2J-1)(2J+3)}, \tag{10a}$$

$$\Delta W_1=-\tfrac{1}{4}\Delta\alpha\langle\vec{E}\cdot\vec{E}\rangle\frac{2J(J+1)+2M^2-2}{(2J-1)(2J+3)}, \tag{10b}$$

indicate that each rotational level is shifted down in energy in the presence of an optical field (Figs. 1 and 2) since the induced molecular polarization in the direction of the field for a molecule in any state is positive. Furthermore, the average of this negative quadratic Stark shift, over the quantum number M of the rotational sublevels, is independent of the rotational level quantum number J since the sum rule

$$\sum_{M=-J}^{+J}-M^2=-\tfrac{1}{3}J(2J+1)(J+1)$$

is valid. Thus, each level (J) contributes equally to the macroscopic linear polarizability $(\alpha_{\parallel}+2\alpha_{\perp})/3$ per molecule.

Obtaining the nonlinear collisionless refractive-index coefficient n_2 of Eq. (9a) necessitates a calculation of the third term in Eq. (7), $hBc\lambda_2 K^2$, which is the quartic Stark shift in rotational energy. The perturbation result consists of two contributions which arise from a coupling of the J,M rotational energy level to the two neighboring

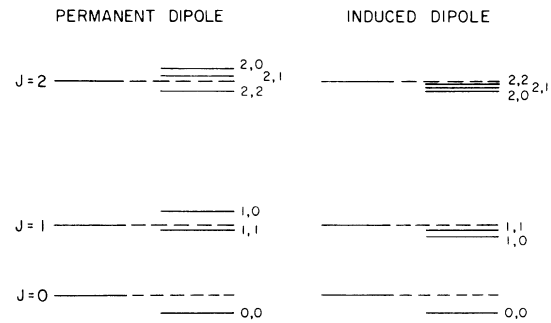

FIG. 1. Lowest Stark-shifted rotational energy levels for a fixed electric field intensity. Those arising from a permanent dipole moment are illustrated on the left-hand side and those arising from the induced dipole moment are shown on the right-hand side. The Stark shifts of the rotational levels due to a permanent dipole moment u are given by[6]

$$\Delta W=\frac{u^2F^2}{hBc}\frac{J(J+1)-3M^2}{J(J+1)(J-1)(2J+3)},$$

where F is the amplitude of the low-frequency or dc field.

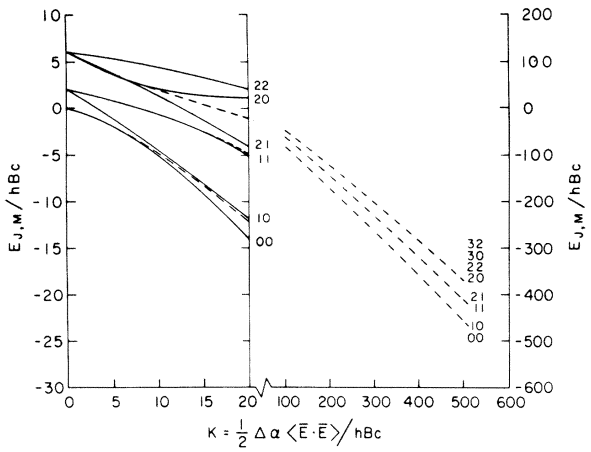

FIG. 2. Stark-shifted rotational energy levels arising from the polarizability anisotropy plotted as a function of $K=\Delta\alpha\langle\vec{E}\cdot\vec{E}\rangle/(2hBc)$. Solid lines indicate the energy shifts obtained from the power series approximation and dotted lines show that obtained from numerical calculations.[9] Note that different scales are used for the low-intensity region and the saturated region.

rotational states satisfying $\Delta J=\pm 2$, $\Delta M=0$, as determined by the selection rules for the $\cos^2\theta$ dependence of the induced dipole moment. This contribution to the induced energy shift of the rotational state J,M can be interpreted as a mutual repulsion of these coupled states. After carrying out the tedious algebraic multiplication and factorization required to combine and simplify the two separate terms given in Ref. 5, one can express the quartic shift as

$$\Delta W_2 = hBcK^2\lambda_2 = hBcK^2\,\frac{M^4P(J)-M^2Q(J)+R(J)}{(2J-3)(2J-1)^3(2J+3)^3(2J+5)}, \tag{11}$$

where

$$P(J)=40J^2+40J+66,$$
$$Q(J)=48J^2+96J^3-4J^2-52J+60,$$
$$R(J)=8J^6+24J^5-6J^4-52J^3+4J^2+34J-6.$$

This is the most important term in the series expansion of the energy shift due to the optical field. In Fig. 2, in which the energy levels of several of the lower rotational states are plotted as a function of the perturbation parameter K, the curvature near $K=0$ gives the quartic Stark shift. This can be either positive or negative depending upon the particular energy state.

Although a relatively complicated expression, the sum of the quartic Stark shifts over the projected quantum number M, which enters into the most important nonlinear coefficient n_2, is particularly simple. This can be conveniently obtained from Eq. (8) and is expressed as

$$F_2(J)=\sum_{M=-J}^{J}\lambda_2=-\frac{1}{60}\left(\frac{1}{(2J-1)^2}-\frac{1}{(2J+3)^2}\right). \tag{12}$$

Higher-order terms in the perturbation expansion are necessary to describe the rotational-energy-level shifts for optical intensities such that $K\gg 1$. Computer multiplication and factorization programs were employed to express the next two orders, λ_3 and λ_4, in the form included in Appendix A, which is convenient for deducing the sum rules. It will be apparent that many more terms are required for an adequate description of such a saturated case, except for the low-temperature limit when only the ground state is significantly populated. This presents major computational difficulties which have not been pursued.

λ_3 and λ_4 simplify considerably when the sums over M are taken. If the results are expanded as a partial-fraction expansion, one obtains

$$F_3(J)=\sum_{M=-J}^{J}\lambda_3 = \frac{1}{210}\left(\frac{1}{(2J-1)^2}-\frac{1}{(2J+3)^2}-\frac{1}{(2J-1)^4}+\frac{1}{(2J+3)^4}\right), \tag{13}$$

$$F_4(J)=\sum_{M=-J}^{J}\lambda_4 = \frac{1}{5040}\left(\frac{9}{16(2J-1)^2}-\frac{9}{16(2J+3)^2}+\frac{59}{4(2J-1)^4}-\frac{59}{4(2J+3)^4}-\frac{15}{(2J-1)^6}+\frac{15}{(2J+3)^6}-\frac{9}{32(2J-3)^2}+\frac{9}{32(J+5)^2}\right). \tag{14}$$

Using the sum rules, Eqs. (12)–(14), the sums $N_i(\eta)$ in Eq. (8) can be handled with relative simplicity, at least numerically. Calculations of $N_2(\eta)$, $N_3(\eta)$, and $N_4(\eta)$ are shown as functions of η in Fig. 3, along with the factor $Z\eta$.

Particularly simple analytical expressions can be obtained for n_2, n_4, and n_6 in the low-temperature limit ($\eta>2$). The nonlinearity in the refractive index is then determined solely by the Stark shift of the ground state, and the coefficients of the refractive-index change are approximately equal to

$$n_2 = \frac{4\pi N}{135}\frac{(\Delta\alpha)^2}{hBcn_0}, \tag{15a}$$

$$n_4 = \frac{6\pi N}{8505}\frac{(\Delta\alpha)^3}{(hBc)^2 n_0}, \tag{15b}$$

$$n_6 = -\frac{26\pi N}{1\,913\,625}\frac{(\Delta\alpha)^4}{(hBc)^3 n_0}. \tag{15c}$$

Since n_6 is negative, the saturation of the refractive index with an increasing optical-field intensity is well approximated by these three coefficients as illustrated in Fig. 4. The saturated value of 4.9 at $K \cong 50$ is close to the expected value for complete alignment in the direction of the field, which is 4.2.

The other extreme, that of the high-temperature limit ($\eta < 0.01$) is applicable to many molecular gases at room temperature (for CS_2 at $T = 300\,^{\circ}\mathrm{K}$, $\eta \simeq 5\times10^{-4}$). In this limit, $Z\eta \simeq 1$ and $N_2(\eta)$ can then be approximated by

$$N_2(\eta) \simeq \sum_{J=0}^{\infty}\sum_{M=-J}^{J}\lambda_2$$

which from Eq. (12) is $-\frac{1}{30}$. Thus,

$$n_2 = (2\pi N/30)\,\Delta\alpha^2/kTn_0. \tag{16}$$

This value of n_2, which arises entirely from the quartic Stark shifts, is a factor of $\frac{3}{4}$ smaller than the usual thermal equilibrium value,[3] which has contributions from the quadratic shift as well (Appendix B).

The similarity of this expression to the thermal equilibrium expression and in particular to the lack of dependence on the quantized behavior of the gas suggests that Eq. (16) is, in principle, derivable from a classical description of the molecular interaction with the field. This calculation appears to be extremely difficult since the absence of thermodynamic equilibrium implies that the nonlinear equations of motion for each molecule would have to be solved explicitly, and an orientational average then taken.

Useful analytical expressions for n_4 and n_6 are much more difficult to obtain in the high-temperature limit. From Eqs. (13) and (14) the sums of the sixth- and eighth-order Stark shifts over all the levels are both zero, since

$$\sum_{J=0}^{\infty} F_3(J) = \sum_{J=0}^{\infty} F_4(J) = 0.$$

This is also apparent from Fig. 3. Thus, in contrast to the case of n_2, for which the Boltzmann factor could be assumed equal to 1 for all terms in $N_2(\eta)$, the deviation of the Boltzmann factor from unity in $N_3(\eta)$ and $N_4(\eta)$ must be considered in order to obtain analytical expressions for n_3 and n_4. Expansion of the Boltzmann factor in terms of η results in divergent series in the sums over J and hence is not useful. However owing to the compensating Stark shifts, without additional higher-order coefficients the terms n_4 and n_6 do not specify the saturated behavior. Hence, we shall not pursue these problems further.

With regards to a more accurate description of the refractive-index saturation, one might consider a numerical calculation the Stark-shifted energy eigenvalues for a strong perturbation. Such calculations have been attempted. However, these have been restricted to rotational levels for $J \leq 10$ which is insufficient for an evaluation of the nonlinear refractive index.

Stern[8] obtained numerical solutions for the en-

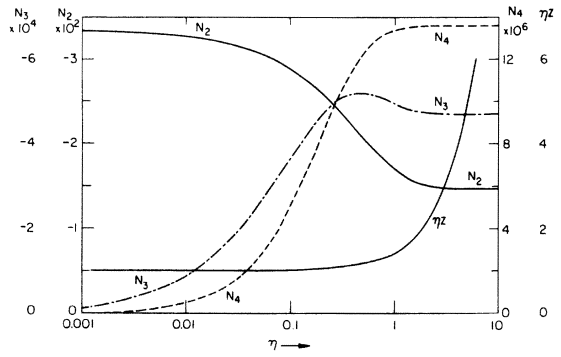

FIG. 3. Nonlinear coefficients $N_2(\eta)$, $N_3(\eta)$, and $N_4(\eta)$ and the factor ηZ plotted as a function of $\eta = hBc/kT$.

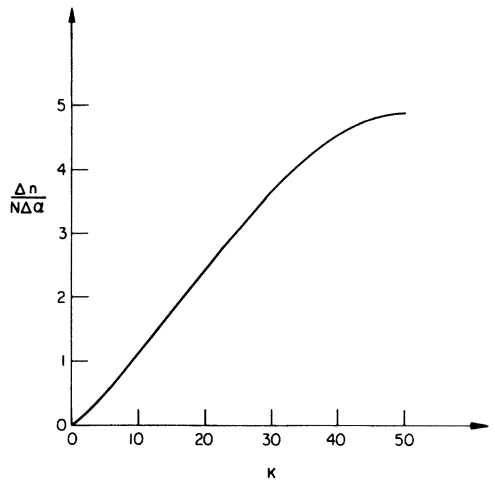

FIG. 4. Saturation of the induced refractive index at low temperatures for a collisionless gas. $\Delta n = n - n_0$ and K is the perturbation parameter $\frac{1}{2}\Delta\alpha\langle\vec{E}\cdot\vec{E}\rangle/hBc$.

ergy levels by solving for the roots of an implicit continued-fraction expansion of the energy eigenvalues. However, these roots are also extremely difficult to determine for large values of the perturbation parameter ($K \gg 20$). These results have been extended by Curl *et al.*[9] by combining a numerical diagonalization of the approximated Hamiltonian matrix with the results of the continued-fraction expression. In this manner, they are able to evaluate the perturbed energy for some lower-energy levels for values of K up to 500.

The Stark shifts for a few rotational energy levels obtained both by the power-series approximation including perturbation terms up to λ_4 and numerically by Curl *et al.* are plotted in Fig. 2. For $K \leq 10$, for which the power series is quite close to the results obtained numerically, the motion of molecules can be described as "rotational." As the perturbing energy is increased, however, the molecular rotation is hindered and eventually the motion is more properly described as "oscillatory."[10] Groups of energy levels merge, each group being characterized by a librational quantum number. (This behavior is indicated on the right-hand side of Fig. 2.) It is apparent that the limiting value of the refractive index is that obtained by total alignment of molecules, $n = 1 + 2\pi N\alpha_{\parallel}$. This is indicated directly in Fig. 2 since the slope of the energy levels asymptotically approach -1 for extremely high electric field intensity.

The most important coefficient to consider experimentally is n_2 since it provides the strength of the various possible nonlinear interactions. This coefficient is given in Table I for several gases of potential interest. For CO_2, CS_2, C_2H_2, and N_2O, n_2 is well approximated by Eq. (16) at 300 °K.

The coefficient for hydrogen at 35 °K and deuterium at 40 °K can be approximated by the low-temperature limit if thermal equilibrium is assumed. Nuclear statistics have been taken into account in the calcuation for N_2 and O_2.[11] Even though these two molecules have relatively small moments of inertia, the results do not differ appreciably from those evaluated from Eq. (5). The index coefficients for HCl and HBr vapors at room temperature were determined by using $N_2(\eta)$ and $Z\eta$ from Fig. 3 in conjunction with Eq. (9).[12]

IV. FIRST-ORDER DENSITY MATRIX CALCULATION OF TIME-DEPENDENT REFRACTIVE-INDEX CHANGES OF GASES COMPOSED OF SYMMETRIC-TOP MOLECULES

In many cases pulsed optical or infrared excitation of vapors composed of anisotropically polarizable molecules will produce a refractive-index change which is quite well described by the stationary results during the excitation. In addition to this adiabatic portion of the response, however, quantum-mechanical interference occurs. This is appreciable if the frequency spectrum of the pulse intensity overlaps many rotational transitions and results in an index of refraction subsequent to the excitation. For many di- and tri-atomic molecular vapors excited by pulses typical of the mode-locked glass laser, an intermediate regime in which both the adiabatic and quantum interference effects are present is expected.

In the present section we wish to introduce two generalizations of the previous results to treat

TABLE I. Nonlinear coefficient n_2 for collisionless gases composed of linear molecules.

	Temperature (°K)	$\Delta\alpha$ (10^{-25} esu)	B (cm^{-1})	n_2 (10^{-12} esu/mole)
CS_2	300	75.0 [a]	0.1092 [d]	171.0
CO_2	300	20.3 [b]	0.3902 [d]	12.6
C_2H_2	300	27.9 [b]	1.177 [d]	23.7
N_2O	300	27.9 [b]	0.4116 [d]	23.7
N_2	300	9.3 [b]	2.001 [e]	2.56
O_2	300	11.4 [b]	1.438 [e]	3.94
HCl	300	7.4 [b]	10.44 [e]	1.53
HBr	300	9.1 [b]	8.360 [e]	2.35
H_2	35	3.02 [c]	59.30 [e]	0.434
D_2	39	2.92 [c]	29.90 [e]	0.803

[a] R. Y. Chiao, E. Garmire, and C. H. Townes, Phys. Rev. Lett. 13, 479 (1964).
[b] Reference 16.
[c] K. B. MacAdam and N. F. Ramsey, Phys. Rev. A 6, 898 (1972).
[d] Reference 17.
[e] Reference 11.

the experimentally expected behavior for a variety of vapors. Firstly, the time dependence in the nonlinear refractive-index change will be treated by utilizing the density matrix equations for the rotational motion. The calculation will, however, only be carried out for the lowest order in the optical intensity so that saturation will not be considered. Secondly, the rotational inertia along the figure axis as well as that perpendicular to the figure axis will be considered to include the more general class of symmetric-top molecules. This additional inertia is expressed through additional terms in the unperturbed Hamiltonian. As for the special case of linear molecules, the polarizability is still specified by two components: $\alpha_{\parallel}$, parallel to the figure axis and $\alpha_{\perp}$, perpendicular to the figure axis. As a result, the directionally dependent, perturbing Hamiltonian is the same as for linear molecules.

In Sec. V the stationary limit of the general time-dependent susceptibility change is obtained. This will provide n_2 for symmetric molecules. The presence of the additional states as specified by the quantized component $\hbar\Lambda$ along the figure axis considerably complicates the perturbation calculation for the stationary Stark shifts. Although the quartic Stark shifts are obtained with relative ease, obtaining terms of any higher order is extremely cumbersome. In addition, numerical calculations of the highly perturbed rotational states have apparently not been attempted thus far.

In Sec. VI we specialize the discussion to the temporal development of the quantum interference exhibited by the collection of evolving superposition states induced by a sufficiently short excitation.

To proceed with the calculation of the refractive-index change for symmetric-top molecules, we denote the element of the density matrix between two rotational states specified by the quantum numbers I, M, Λ, and J, M, Λ by $\rho_{I,J}$. In analogy to linear molecular gases, the quantum numbers M and Λ need not be considered explicitly. However, it must be kept in mind that whenever a sum arises it is to be taken over M and Λ as well as J.

The equations of motion for the density matrix are[13]

$$\frac{\partial \rho_{I,J}}{\partial t} = \frac{i}{\hbar} \sum_{K} (\rho_{I,K} H_{K,J} - H_{I,K} \rho_{K,J}), \tag{17}$$

where $H = H^0 + H'$ is the total Hamiltonian, H' being specified by expression (2) or (4), depending on the polarization. From this point on, we will specifically discuss linear polarization.

The matrix elements of H^0, the unperturbed energy eigenvalues, are[6,11]

$$H^0_{J,\Lambda} = hBcJ(J+1) + hc(A-B)\Lambda^2, \tag{18}$$

where A and B are, respectively, the rotational constant about the figure axis and that about the axis perpendicular to the figure axis.

The matrix elements of the perturbing Hamiltonian are $H'_{I,J} = -\frac{1}{2}\Delta\alpha \langle \vec{E} \cdot \vec{E} \rangle Q_{I,J}$. The $Q_{I,J}$, which are the matrix elements for the operator $\cos^2\theta$, can be obtained by using the table given by Cross *et al.*[14] These matrix elements are

$$Q_{J,J-2} = \frac{1}{J(J-1)(2J-1)} \left(\frac{(J^2-M^2)(J^2-\Lambda^2)[(J-1)^2-M^2][(J-1)^2-\Lambda^2]}{(2J-3)(2J+1)} \right)^{1/2}, \tag{19a}$$

$$Q_{J,J+2} = \frac{1}{(J+1)(J+2)(2J+3)} \left(\frac{[(J+2)^2-M^2][(J+2)^2-\Lambda^2][(J+1)^2-M^2][(J+1)^2-\Lambda^2]}{(2J+1)(2J+5)} \right)^{1/2}, \tag{19b}$$

$$Q_{J,J} = \frac{(J^2-M^2)(J^2-\Lambda^2)}{J^2(2J-1)(2J+1)} + \frac{[(J+1)^2-M^2][(J+1)^2-\Lambda^2]}{(J+1)^2(2J+1)(2J+3)} + \frac{M^2\Lambda^2}{J^2(J+1)^2}, \tag{19c}$$

where Λ and M are not included explicitly as indices on the Q terms since they remain unchanged during a transition.

The refractive index can be determined from the induced susceptibility which is obtained from the trace of the product of the operator $N(\Delta\alpha \cos^2\theta + \alpha_{\perp})$ and the density matrix obtained from Eq. (17).

The zeroth order of approximation gives the linear refractive index n_0, which depends only on the values of the density-matrix elements prior to the optical disturbance. One readily finds that

$$n_0 = (2\pi N/3)(\alpha_{\parallel} + 2\alpha_{\perp})$$

in agreement with the theorem of spectroscopic stability[15] and the previous result from the quadratic Stark shifts.

The lowest-order values for the off-diagonal components of the density matrix and the corresponding nonlinear refractive-index change can be obtained immediately by replacing the $Q_{I,J}$ in the results for linear molecules in Ref. 4 by those of Eq. (19). Since the quantum number Λ as well as

M does not change during a rotational transition, the only difference in the final results is an additional sum over the quantum number Λ. Thus the expressions for $\rho_{J+2,J}$ and Δn (Ref. 4) are rewritten:

$$\rho_{J+2,J} = -i\left(R_{J+2,J}\int_{t_0}^{t}\exp(-i\omega_J t')\langle\vec{E}\cdot\vec{E}\rangle\,dt'\right)\times\exp(i\omega_J t), \tag{20a}$$

$$\rho_{J,J+2} = \rho^*_{J+2,J}, \tag{20b}$$

$$\Delta n(t) = \frac{4\pi N}{n_0}\sum_{J=0}^{\infty} T_J \mathrm{Im}\left(e^{i\omega_J t}\int_{t_0}^{t} e^{i\omega_J t'}\langle\vec{E}\cdot\vec{E}\rangle\,dt'\right), \tag{21}$$

where t_0 is an initial time for which $\langle\vec{E}\cdot\vec{E}\rangle$ can be assumed to be zero. T_J is the double sum

$$T_J = \sum_{M,\Lambda=-J} R_{J+2,J}Q_{J+2,J}\Delta\alpha, \tag{22}$$

with $\omega_J = 4\pi Bc(2J+3)$ and Im, the imaginary part of the term inside the parentheses. As previously,

$$R_{J+2,J} = [(\rho^{(0)}_{J,J} - \rho^{(0)}_{J+2,J+2})/2\hbar]Q_{J+2,J}\Delta\alpha, \tag{23}$$

where $\rho^{(0)}_{J,J}$ is the initial zero-field thermal equilibrium value of the diagonal component of the density matrix:

$$\rho^{(0)}_{J,J} = \exp(-H^0_{J,\Lambda}/kT)\Big/\sum_{J=0}^{\infty}\sum_{\Lambda=-J}^{J}(2J+1)\exp(-H^0_{J,\Lambda}/kT). \tag{24}$$

In the above expression for T_J, the sum over M can be explicitly carried out, giving

$$T_J = \frac{(\Delta\alpha)^2}{15\hbar}\sum_{\Lambda=-J}^{J}\left(\rho^{(0)}_{J,J} - \rho^{(0)}_{J+2,J+2}\right)\times\frac{[(J+1)^2-\Lambda^2][(J+2)^2-\Lambda^2]}{(J+1)(J+2)(2J+3)}. \tag{25}$$

This obviously reduces to the results for a linear molecular gas when $\Lambda = 0$.[4]

V. STATIONARY REFRACTIVE-INDEX CHANGE FOR SYMMETRIC-TOP MOLECULAR GASES

To evaluate the stationary intensity-dependent refractive index from Eq. (21), it is assumed that $\langle\vec{E}\cdot\vec{E}\rangle$ is slowly varying with respect to $e^{-i\omega_J t}$ and that $\langle\vec{E}\cdot\vec{E}\rangle$ is zero for $t' = t_0$. Integrating Eq. (21) by parts and neglecting time derivatives of $\langle\vec{E}\cdot\vec{E}\rangle$, one obtains for any given time t:

$$\Delta n = \frac{4\pi N}{n_0}\sum_{J=0}^{\infty}\frac{T_J}{\omega_J}\langle\vec{E}\cdot\vec{E}\rangle, \tag{26}$$

which is a generalization of Eq. (9) obtained for linear molecules using the time-independent approach.

In the low-temperature limit, Eq. (26) reduces to (15a) since only the level with the lowest energy $E(J=0,\Lambda=0,M=0)$ is populated. In the high-temperature limit, no analytic expression analogous to Eq. (15) can be deduced with assumptions corresponding to those employed for linear molecules. The expression for the induced refractive-index change in this case can be conveniently written:

$$\Delta n = F(T)\left(\frac{2\pi N}{30}\frac{(\Delta\alpha)^2}{kTn_0}\right)\langle\vec{E}\cdot\vec{E}\rangle. \tag{27}$$

The coefficient $F(T)$, in general, depends on temperature and on the rotational constants A and B. Numerical calculations have been made for the CH_3Cl molecule, which has polarizabilities $\alpha_\parallel = 5.42\times10^{-24}$ esu and $\alpha_\perp = 4.14\times10^{-24}$ esu,[16] and rotational constants $A = 5.090$ cm^{-1} and $B = 0.4434$ cm^{-1}.[17] Results show that the coefficient $F(T)$ for this molecule is 0.8434 at $T = 296$ °K and 0.8461 at $T = 1000$ °K.

For temperatures high enough for $F(T)$ not to vary significantly (≥ 1000 °K for CH_3Cl), the refractive-index change depends on A and B only through their ratio. This dependence is indicated in Fig. 5. The coefficient $F(T)$ decreases with decreasing A/B to approximately 0.4291 when $A/B = 1/2$, which is the value for an "ideal ring molecule." Such a decrease in the value of $F(T)$ with decreasing A/B results from the combined effect of the decrease in $Q_{I,J}$ with increasing Λ and the decrease of the unperturbed rotational energy with a decreasing A/B. The latter implies that the states with high Λ (and hence low values of $Q_{I,J}$) are

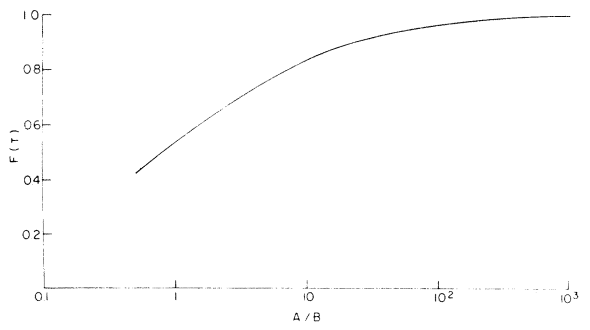

FIG. 5. Dependence of the effective factor $F(T)$ for symmetric-top molecules on the ratio of the rotational constants A and B. These were evaluated for the high-temperature limit ($T = 1200$ °K, $B = 0.1092$ cm^{-1}) for which $F(T)$ depends only on A/B.

weighted more heavily in the sum over Λ in Eq. (26).

The coefficient n_2 and the factor $F(T)$ of several symmetric-top molecular gases are given in Table II.

VI. COHERENT TIME-DEPENDENT REFRACTIVE-INDEX CHANGES IN GASES COMPOSED OF SYMMETRIC-TOP MOLECULES

The rotational response of a molecular gas to an optical pulse exhibits a non-negligible explicit time dependence if the pulse duration is not too long. For symmetric-top molecules, such will be the case for durations less than or equal to the inverse of the fundamental quadrupole transition frequency, which is $1/6\,Bc$. The spectral content of the pulse envelope then overlaps the rotational transition frequencies and a significant number of transitions can occur among the Stark-shifted rotational states evaluated in Sec. II. These transitions are, of course, not taken into account in the stationary perturbation calculations.

The transitions result in a net absorption of energy by the gas, leaving the rotational population distribution, and hence the refractive index, perturbed after the passage of the pulse.

Such a perturbation can also be interpreted in terms of a transient development, during the optical excitation, of superpositions of pairs of rotational states. At the termination of the excitation, the percentage of each state composing the pair ceases to change, while the relative phase between the two states continues to evolve at a constant rate equal to the transition frequency between the two.

The nonlinear refractive-index change subsequent to the optical excitation is described by a collection of such steady-state superposition states, each of which is thus evolving with a well-established phase relationship with respect to the remaining superposition states. The collection is expressed by a Fourier sum that has components at the quadrupole transition frequencies $\omega_J = 4\pi Bc(2J+3)$. Such a sum is obtained from Eq. (21) by extending the upper limit to infinity, this being justified since $\langle \vec{E}\cdot\vec{E}\rangle$ is zero for all t subsequent to excitation.

The Fourier component for a particular frequency ω_J is the product of the Fourier transform of the optical intensity at frequency ω_J and the coefficient T_J defined by Eq. (25). For linear molecules for which the sum over Λ can be dropped and Λ set to equal to zero, the Fourier sum over the rotational frequency spectrum has been shown to represent short periodic bursts in the refractive index, spaced in time by intervals of $1/4Bc$.[4]

A complete analysis of the excited refractive-index change, in particular one that includes the response during excitation with the optical pulse and the strength of the subsequent short bursts as a function of pulse width, requires a numerical integration of Eq. (21). Figure 6 illustrates the overall features of the time-dependent refractive-index change. This particular example pertains to CS_2 vapor ($A \to \infty, B = 0.1091\ \mathrm{cm}^{-1}$)[17] for an optical excitation assumed to have a Gaussian electric-field profile given by

$$E = \tfrac{1}{2}A \exp(-2t^2/\tau^2)(e^{i\omega t} + e^{-i\omega t}). \tag{28}$$

For a relatively long pulse (5 psec or longer), the initial refractive-index change closely follows that given by the stationary quartic Stark shift (hence, the pulse shape), and the strength of the quantum interference is small compared to that of this initial response. With a reduction in the pulse width (1 psec or shorter), the refractive-index change occurring simultaneously with the excitation diminishes. The initial response gradually attains the time profile expected of the burst due to quantum interference. When pulse width τ becomes much less than the width of the bursts in refractive index, the entire index change is completely described by the sum over the fully developed or steady-state superposition states.

For symmetric-top molecules, the particular Fourier series describing only the refractive index subsequent to excitation by a Gaussian field described by Eq. (28), as determined from Eq. (21), is

TABLE II. Nonlinear coefficient n_2 for collisionless gases composed of symmetric-top molecules at 296 °K.

	A [a] (cm^{-1})	B [a] (cm^{-1})	$\Delta\alpha$ [b] (10^{-25} esu)	$F(T)$	n_2 (10^{-12} esu/mole)
CH_3Cl	5.090	0.4434	12.8	0.843	4.27
C_2H_6	2.538	0.6621	15.1	0.722	5.09
C_6H_6	0.0948	0.1896	−59.6	0.429	47.0
NH_3	6.196	9.444	2.40	0.436	0.0776

[a] See Ref. 17. [b] See Ref. 16.

$$\Delta n(t) = \pi^{3/2} N \tau A^2 \sum_{J=0}^{\infty} T_J \exp(-\omega_J^2 \tau^2/16) \sin\omega_J t. \tag{29}$$

In general, the width and shape of the bursts in the refractive-index change depend on the width of the excitation pulse as well as the spectral content of the coefficients T_J. When the pulse is very short so that the Fourier spectrum is essentially constant over the dominating rotational transition frequencies, the spectral content of the refractive index is limited by the spectral width of T_J. The relative amplitude of T_J as a function of J is plotted in Fig. 7 for CS_2 vapor at 296 °K. The effective rotational levels range roughly from $J=20$ to 70, which gives a bandwidth of $\Delta f = 4Bc(70-20) = 6.5\times10^{11}$ sec^{-1}. Hence, the width of the complete burst, covering both the positive peak and the negative peak, is approximately $\Delta\tau = 1/\Delta f = 1.5\times10^{-12}$ sec. The full width of either peak at half the maximum amplitude is about $\frac{1}{3}$ of this value or 0.5×10^{-12} sec.

For the opposite extreme, that of a pulse having a spectral width for which only relatively few of the thermally populated energy levels are excited, the width of the burst is roughly proportional to the pulse width.

Both extremes in excitation pulse width, extremely short or extremely long, produce a small number of superposed states and consequently quantum interference strength. The most efficient utilization of a burst of optical energy occurs when it is contained in a time duration that is roughly the inverse of the frequency of the dominating rotational transitions. Since for large J, for linear molecules, T_J is approximately proportional to $J^2\exp(-J^2hBc/kT)$, the level with the maximum value for this factor is given by $J_{max} = (kT/hBc)^{1/2}$, which for CS_2 at 296 °K is approximately 44.[4] The optimum pulse width is the inverse of $4BcJ_{max}$:

$$\tau_{op} \simeq \frac{1}{4Bc}\left(\frac{hBc}{kT}\right)^{1/2} = 5\times10^{-12}(BT)^{-1/2}. \tag{30}$$

A numerical calculation over a temperature range 100–1200 °K for different values of B gives $\tau_{op} = 4.5\times10^{-12}\ (BT)^{-1/2}$ in close agreement with this approximation expression. Figure 8, in which the peak amplitude of the refractive index in CS_2 $1/4Bc$ after excitation is plotted as a function of excitation-pulse duration, illustrates the range about the optimum pulse width which can be tolerated without decreasing the strength of the echo significantly.

Computed refractive-index profiles due to quantum interference induced by Gaussian-shaped light beams in CS_2 vapors and CH_3Cl vapors at 296 °K are plotted in Fig. 9 for various pulse widths. One notes that the normalization constant for the latter

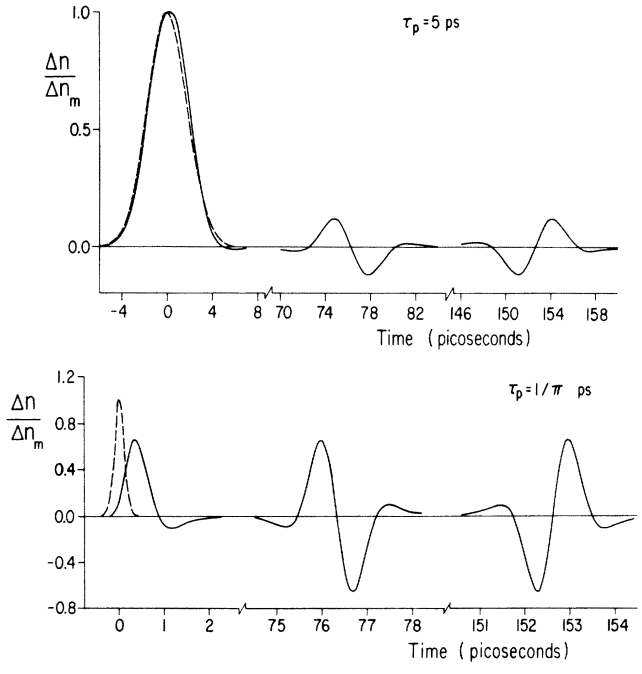

FIG. 6. Theoretically predicted time variation of the refractive-index change induced by a Gaussian-shaped optical pulse in CS_2 vapor at 296 °K. The pulse widths τ as defined by Eq. (28) for the individual curve are (a) $\tau = 5\times10^{-12}$ sec. The curves are normalized with respect to $\Delta n_m = (2\pi N/30n_0)(\Delta\alpha)^2A^2/2kT$ (which is 1.74×10^{-10} $A^2/2$ esu/mole). (b) $\tau = (1/\pi)\times10^{-12}$ sec.

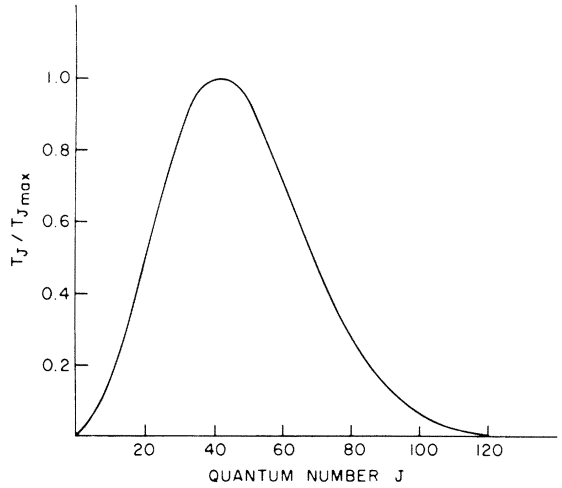

FIG. 7. Amplitudes of the coefficient T_J for CS_2 vapor at 296 °K. The curve is normalized with respect to the maximum coefficient $T_{J_{max}}$, where $J_{max}=42$.

is $\Delta n_s = F(T)[2\pi N(\Delta\alpha)^2/30kTn_0]$, with $F(T) = 0.8434$.

Comparing Fig. 9(a) with 9(b), we see that the time profiles are almost the same for the linear and symmetric-top molecules. They are both antisymmetric since the fundamental frequency of the Fourier components in both cases is $2B$ and the function is odd. On the other hand, for the symmetric top, the normalized refractive-index change can be larger than unity in contrast to that of the linear molecule. For CH_3Cl vapor, it is 1.08 at room temperature. However, since $\Delta n_\epsilon = 0.843\ \Delta n_m$, the amplitude is still smaller than that of a linear molecule having the same rotational constant B and the same polarizability anisotropy $\Delta\alpha$. In addition, for the symmetric-top molecule, the level of maximum contribution tends to have a high J value and hence an optimum pulse width shorter than that of the linear molecule. Consequently, the width of the burst is also shorter for the symmetric-top molecule. [This width cannot be computed from Eq. (30).]

Table III lists the optimum pulse widths and echo periods for several gases at 296 °K. The widths have been obtained from Eq. (30) for linear molecules and numerically for the remaining ones. CS_2 and benzene appear particularly favorable for initial investigations. They both have large anisotropies and relatively small rotational constants and require optimum pulse widths that could be achieved with present mode-locked lasers.

Interference with the rotational coherence will arise from collisional and Doppler effects. Significantly populated excited vibrational levels as well as the centrifugal stretching parameter could also interfere with the rotational coherence, provided the rotational constants vary significantly.

For CS_2, the rotational constant is hardly effected by contrifugal stretching (for the level with

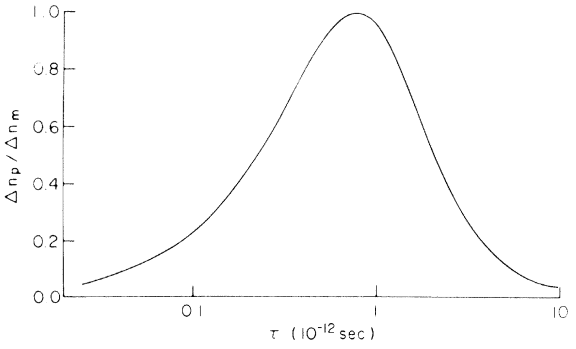

FIG. 8. Normalized peak amplitudes of the refractive index Δn_p of the refractive-index burst for a time delay $1/4Bc$ after excitation for CS_2 vapor at 296 °K as a function of the excitation pulse width [defined by Eq. (28)]. The normalization is as for Fig. 6.

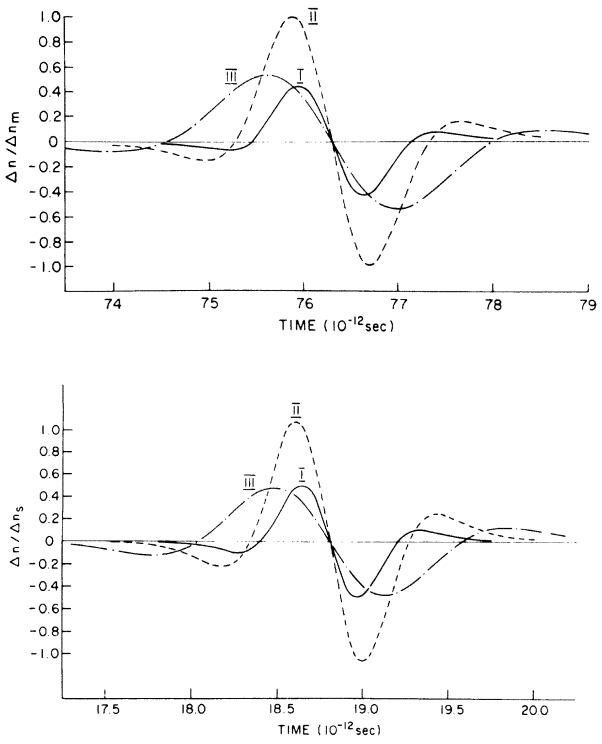

FIG. 9. Theoretically predicted refactive-index bursts induced by Gaussian-shaped optical pulses. (a) Bursts in CS_2 vapor at 296 °K. The normalization is as for Fig. 6. The excitation pulse widths are (I) $\tau = 0.2\times10^{-12}$ sec, (II) $\tau = 0.8\times10^{12}$ sec, and (III) $\tau = 2\times10^{-12}$ sec. (b) Bursts in CH_3Cl vapor at 296 °K. The normalization constant is $\Delta n_s = F(T)(2\pi N/30n_0)\times[(\Delta\alpha)^2A^2/2kT]$ where $F(T) = 0.843$ (equal to $4.27\times10^{-12}A^2/2$ esu/mole). The excitation pulse widths are (I) $\tau = 0.1\times10^{-12}$ sec, (II) $\tau = 0.37\times10^{-12}$ sec, and (III) $\tau = 10^{-12}$ sec.

TABLE III. Time separation between refractive-index bursts and the optimum width of the optical excitation at 296 °K.

	$\tau_d = 1/4Bc$ (10^{-12} sec)	τ_{op} (10^{-12} sec)
CS_2	76.32	0.80
CO_2	21.37	0.42
N_2O	20.26	0.41
CH_3Cl	17.02	0.35
C_2H_6	12.59	0.29
C_6H_6	43.98	0.47

$J=200$, the increase in rotational constant is 0.01%). In addition, the rotational constant of the vibrationally excited molecules is barely different from that of the unexcited ones. Hence, though 11% of the molecules are in the first excited state, the induced refractive index should not be changed appreciably. Note that the lowest vibrational levels of benzene is above the highly populated rotational levels. In addition, the small centrifugal-stretching parameters coupled with a small rotational constant and a large anisotropy in polarizability make this particularly favorable as well.[18]

VII. INTEGRATED STRENGTH AND DETECTION OF THE REFRACTIVE-INDEX RESPONSE

Although the amplitude of the refractive-index change subsequent to optical excitation is highly dependent on the optical pulse duration, the time integration of the entire induced-refractive index response depends only on the energy of the exciting pulse and not on its duration.

From expression (21), the total area A_T is given by

$$A_T=\frac{4\pi N}{n_0}\sum_{J=0}^{\infty}T_J\,\mathrm{Im}\left[\int_{-\infty}^{\infty}e^{i\omega_J t}\int_{-\infty}^{t}\langle\vec{E}\cdot\vec{E}\rangle\,e^{i\omega_J t'}\,dt'\,dt\right]. \tag{31}$$

For generality, $\langle\vec{E}\cdot\vec{E}\rangle$ is assumed to have an arbitrary time profile, although Gaussian-shaped pulse envelopes are reasonably justified for most Q-switched and perhaps mode-locked laser pulses. Rather than obtaining a delayed refractive-index burst that is antisymmetric about its center of gravity, Eq. (21) shows that the asymmetric part of the optical pulse gives rise to a superposed contribution that is symmetric about the center of gravity. For example, Fig. 10 illustrates a sequence of bursts induced in CS_2 gas at room temperature by an optical excitation with both symmetric and antisymmetric components of the intensity as specified by

$$\langle\vec{E}\cdot\vec{E}\rangle=A_0(t)+A_e(t), \tag{32a}$$

where

$$A_0(t)=C_1\exp[-4(t+\tfrac{1}{4}\tau)^2/\tau^2]-\exp[-4(t-\tfrac{1}{4}\tau)^2/\tau^2], \tag{32b}$$

$$A_e(t)=C_2\exp[-4t^2/\tau^2], \tag{32c}$$

and C_1 and C_2 are constants.

It is evident that the net contribution to the total time-integrated refractive-index change is zero subsequent to $t=(8Bc)^{-1}$ for the portion of the excitation which is an even function of t and subsequent to $t=(4Bc)^{-1}$ for that which is an odd function of t. Thus we need consider only times less than these for the two contributions, respectively. Changing the order of integration for each of these in Eq. (31) and explicitly carrying out the integration with respect to t, one obtains

$$A_T=\frac{4\pi N}{n_0}\sum_{J=0}^{\infty}\frac{T_J}{\omega_J}\left(\int_{-\infty}^{1/8Bc}A_e(t')\,dt'+\int_{-\infty}^{1/4Bc}A_0(t')\,dt'\right)-\frac{4\pi N}{n_0}\sum_{J=0}^{\infty}\frac{T_J}{\omega_J}\left(\int_{-\infty}^{1/8Bc}A_e(t')\sin\omega_J t'\,dt'+\int_{-\infty}^{1/4Bc}A_0(t')\cos\omega_J t'\,dt'\right). \tag{33}$$

If the pulse width τ is shorter than $(8Bc)^{-1}$, where τ is the full width at half intensity, the upper limit of the integration can be extended to infinity. From symmetry, the second set of bracketed terms vanishes after the integration. The total area reduces to

$$A_T=\frac{4\pi N}{n_0}\sum_{J=0}^{\infty}\frac{T_J}{\omega_J}\int_{-\infty}^{\infty}\langle\vec{E}\cdot\vec{E}\rangle\,dt, \tag{34}$$

which is just the total area that would be obtained from a stationary calculation.

The upper integration limits can be taken without loss of generality as $1/8Bc+n/2Bc$ and $1/4Bc+n/2Bc$, respectively, for even and odd components of the excitation, where n is a positive integer. Thus, Eq. (33) is applicable for pulses of duration $(8Bc)^{-1}$ or larger. However, for pulses having such a long duration, the strength of the quantum

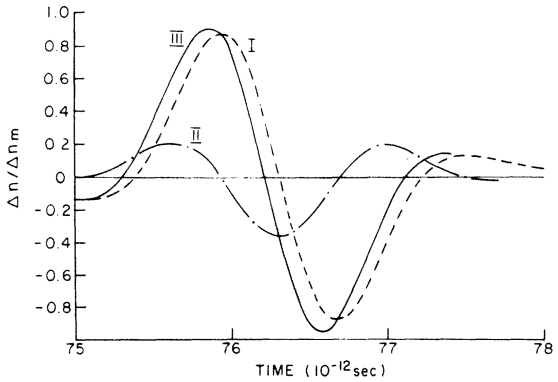

FIG. 10. Illustration of refractive-index bursts induced by an optical pulse whose intensity is not symmetric about any time. CS_2 at 296 °K has been assumed; Δn_m is the same as for Fig. 6 but with $A^2=C_2^2$. (I) The contribution to the burst by the portion of the optical pulse that is an even function of time [Eq. (32)]. (II) The contribution due to the portion that is an odd function of time [Eq. (32) with $C_1=0.4C_2$], and (III) the total theoretically predicted burst.

TABLE IV. Detectability of refractive-index bursts for gases at 1 atm pressure for a propagation length of 1 m. The peak electric field intensity of the inducing optical pulse is assumed to be 2×10^3 esu, and the wavelength of the probe beam is 0.53 μm. $E_\parallel$ is the electric-field component of the probe pulse which is parallel to the electric field of the excitation pulse; $E_\perp$ is that perpendicular to the excitation pulse field.

Substance	Temperature (°K)	Optimum pulse width (10^{-12} sec)	$n_2(T,P)$ (esu/cm^3)	Relative phase shift of $E_\parallel$ and $E_\perp$ $\Delta\phi$ (rad)	Fraction of diode pulse energy transmitted, $(\Delta\phi/2)^2$
CS_2	319	0.77	7.2×10^{-15}	0.26	0.017
N_2O	296	0.41	1.07×10^{-15}	0.038	3.6×10^{-4}
C_6H_6	353	0.43	1.60×10^{-15}	0.057	8.1×10^{-4}
CH_3Cl	296	0.37	1.91×10^{-16}	0.0068	1.2×10^{-15}

interference is negligible and the refractive index is given very well by the stationary result.

The experimental detection of the transient portion of the refractive-index change should, according to the above, roughly depend only on the total energy of the optically exciting pulse. This is true for a detection technique that produces a signal linearly proportional to the birefringence[2] and a probe pulse of the same duration as the birefringence pulse. The recent technique for probing short-duration birefringence employed by Duguay and Hansen[19] involves the square of the birefringence for which the detected signal will increase with a decrease in the exciting pulse width up to the point at which the birefringence becomes independent of the pulse width.

The detectability of the delayed bursts in refractive index for several molecular species is tabulated in Table IV. As for Table III, the optimum length of the excitation pulse has been estimated numerically for symmetric-top molecules and from Eq. (30) for linear molecules. The maximum relative phase shift between the electric field components perpendicular to and parallel to the polarization direction of the excitation pulse and produced by the refractive-index burst has also been listed as $\Delta\phi$. This has been evaluated for a length of 1 m, at a wavelength of 0.53 μm, and for a peak power density of 500 MW/cm^2 for the excitation. The resultant fraction of energy which would be transmitted through an analyzing polarizer has been estimated assuming the probe pulse to be centered on the peak of the refractive-index profile for the 1 m length, and, in addition, that it is much shorter than the duration of the refractive-index profile. Consequently, this is the optimum value that would be obtained. If the probe pulse is of the order of the width of the echoic response then one would expect this to be reduced by approximately a factor of 2.

The resultant signal-to-noise ratios that can be achieved for the rather conservative optical intensity chosen are encouraging. This has been obtained as the ratio of the above percentage of the energy of the probe pulse which is transmitted by the crossed polarizers due to the echoic response to that which would be transmitted in the absence of the echoic response. The latter is primarily determined by the extinction ratio of the polarizer pair, which can be of the order of 10^{-6}. Scattering due to the vapor and the window of the sample cell have not been included but should not present any difficulty.

VIII. CONCLUSIONS

The sequence of refractive-index bursts, which is essentially the rotational response of the molecule to a δ-function excitation, should be useful for various spectroscopic measurements. The spacing between the bursts provides a direct measurement of the rotational constant of symmetric-top molecules. This method would be particularly convenient for relatively large organic molecules that possess a center of inversion, such as pyrene. For conventional spectroscopic approaches, broadening would cause the rotational transitions to merge. In the time domain, however, the bursts are diminished in amplitude due to Doppler or collisional effects but should still be detectable. This result together with the fact that molecules with large moments of inertia exhibit a relatively long ($\simeq 3\times10^{-9}$ sec for pyrene) delay before the appearance of the refractive-index change and an optimum pulse width that is longer ($\simeq 2\times10^{-12}$ sec for pyrene at 296 °K) provide an advantage.

The transient response in the refractive index should also provide a useful means of studying collisional phenomena in gases. Even the factor of $\frac{3}{4}$ reduction of the collisionless stationary value of n_2 with respect to the thermodynamic equilibrium value should be significant enough to be easily detected.

APPENDIX A: LINEAR MOLECULAR STARK SHIFTS

The eigenvalues associated with the spheroidal wave functions have been given in a power-series expansion.[5] To evaluate the refractive index, it is convenient to rewrite the coefficient for each power of the perturbation parameter in terms of a common denominator and to arrange the numerator in a descending series in terms of powers of quantum number M. The first three terms are given in Sec. III; λ_3 and λ_4 are, respectively,

$$\lambda_3 = \frac{Q_6M^6 + Q_4M^4 + Q_2M^2 + Q_0}{(2J-5)(2J-3)(2J-1)^5(2J+1)(2J+3)^5(2J+5)(2J+7)}, \tag{A1a}$$

$$\lambda_4 = \frac{R_8M^8 + R_6M^6 + R_4M^4 + R_2M^2 + R_0}{16(2J-7)(2J-5)^2(2J-3)^3(2J-1)^7(2J+1)(2J+3)^7(2J+5)^3(2J+7)^2(2J+9)}, \tag{A1b}$$

where

$$Q_0 = -4(140J^9 + 720J^8 + 688J^7 - 952J^6 - 1758J^5 - 335J^4 + 798J^3 + 576J^2 + 91J - 15),$$

$$Q_2 = 8(320J^9 + 1440J^8 + 1600J^7 - 1120J^6 - 2172J^5 + 730J^4 + 2106J^3 + 909J^2 + 735J + 315),$$

$$Q_4 = -4(1792J^7 + 6272J^6 + 11040J^5 + 11920J^4 + 6656J^3 + 1200J^2 + 6834J + 3465),$$

$$Q_6 = 16(288J^5 + 720J^4 + 2576J^3 + 3144J^2 + 2410J + 705),$$

$$\begin{aligned} R_0 = {} & 2\,621\,440J^{22} + 28\,835\,840J^{21} + 67\,502\,080J^{20} - 334\,233\,600J^{19} - 1\,652\,391\,936J^{18} + 406\,880\,256J^{17} \\ & + 12\,640\,935\,936J^{16} + 11\,465\,981\,952J^{15} - 47\,151\,794\,176J^{14} - 86\,929\,668\,096J^{13} + 60\,776\,768\,000J^{12} \\ & + 283\,966\,432\,256J^{11} + 179\,093\,012\,352J^{10} - 331\,641\,182\,336J^9 - 597\,523\,865\,568J^8 - 39\,584\,051\,328J^7 \\ & + 562\,799\,872\,768J^6 + 305\,661\,829\,696J^5 - 144\,966\,710\,848J^4 - 144\,459\,953\,280J^3 - 23\,823\,704\,448J^2 \\ & + 1\,681\,374\,240J - 123\,832\,800, \end{aligned}$$

$$\begin{aligned} R_2 = {} & -132\,120\,576J^{20} - 1\,321\,205\,760J^{19} - 2\,986\,868\,736J^{18} + 10\,772\,545\,536J^{17} + 55\,153\,655\,808J^{16} \\ & + 26\,351\,763\,456J^{15} - 230\,151\,454\,720J^{14} - 364\,095\,176\,704J^{13} + 213\,326\,028\,800J^{12} + 709\,242\,830\,848J^{11} \\ & - 39\,055\,316\,992J^{10} - 538\,931\,681\,280J^9 + 423\,846\,592\,000J^8 + 536\,931\,813\,376J^7 - 796\,268\,822\,912J^6 \\ & - 1\,151\,804\,954\,752J^5 - 44\,866\,063\,232J^4 + 732\,693\,962\,880J^3 + 534\,689\,631\,360J^2 + 153\,715\,363\,200J \\ & + 15\,812\,496\,000, \end{aligned}$$

$$\begin{aligned} R_4 = {} & 858\,783\,744J^{18} + 7\,729\,053\,696J^{17} + 16\,658\,989\,056J^{16} - 41\,919\,971\,328J^{15} - 235\,709\,202\,432J^{14} \\ & - 303\,193\,325\,568J^{13} + 358\,526\,828\,544J^{12} + 1\,907\,821\,019\,136J^{11} + 2\,395\,260\,653\,568J^{10} \\ & - 1\,479\,590\,572\,032J^9 - 5\,776\,834\,200\,576J^8 - 1\,235\,455\,438\,848J^7 + 5\,280\,868\,948\,244J^6 \\ & + 1\,601\,948\,246\,784J^5 - 3\,438\,094\,991\,424J^4 - 1\,925\,582\,232\,960J^3 - 1\,295\,953\,634\,304J^2 \\ & - 1\,226\,174\,604\,480J - 338\,863\,694\,400, \end{aligned}$$

$$\begin{aligned} R_6 = {} & -149\,946\,3680J^{16} - 11\,995\,709\,440J^{15} - 28\,251\,258\,880J^{14} + 12\,166\,103\,040J^{13} + 263\,258\,767\,360J^{12} \\ & + 875\,588\,485\,120J^{11} + 691\,770\,327\,040J^{10} - 2\,847\,928\,647\,680J^9 - 6\,429\,128\,499\,200J^8 \\ & - 2\,067\,620\,659\,200J^7 + 5\,728\,792\,217\,600J^6 + 6\,081\,225\,021\,440J^5 + 2\,478\,926\,763\,520J^4 \\ & + 1\,276\,743\,582\,720J^3 + 4\,306\,275\,239\,040J^2 + 3\,691\,965\,916\,800J + 877\,688\,784\,000, \end{aligned}$$

$$\begin{aligned} R_8 = {} & 770\,179\,072J^{14} + 5\,391\,253\,504J^{13} + 15\,384\,051\,712J^{12} + 22\,218\,014\,720J^{11} - 103\,817\,510\,912J^{10} \\ & - 594\,261\,147\,648J^9 - 647\,287\,250\,944J^8 + 1\,000\,544\,829\,440J^7 + 3\,448\,504\,383\,488J^6 + 4\,334\,596\,040\,704J^5 \\ & - 611\,972\,320\,768J^4 - 6\,087\,058\,191\,360J^3 - 6\,531\,288\,018\,048J^2 - 3\,111\,137\,285\,760J - 554\,513\,752\,800. \end{aligned}$$

The last three terms, which give rise to the nonlinear refractive-index change, were discussed in the text. The second term gives the total quadratic Stark shift for each J level. The expectation value is

$$\langle \Delta W_1 \rangle = hBcK \frac{\sum_{J=0}^{\infty} -\frac{1}{3}(2J+1)e^{-J(J+1)\eta}}{\sum_{J=0}^{\infty}(2J+1)e^{-J(J+1)\eta}}$$

$$= -\tfrac{1}{6}\Delta\alpha E^2. \tag{A2}$$

Thus, each J level contributes equally to the linear refractive index, $1+\frac{2}{3}\pi N(\alpha_{\parallel}+2\alpha_{\perp})$.

APPENDIX B: OPTICALLY INDUCED REFRACTIVE INDEX FOR THERMAL EQUILIBRIUM

The intensity-dependent portion of the nonlinear refractive-index change arising from the Stark shifts of the rotational levels, which are assumed to be in thermodynamic equilibrium at temperature T, can be deduced from an average of the perturbed energy. We wish to obtain the high-temperature limit and show that it is equivalent to that given by the classical calculation.

The partition function including the quartic Stark terms is given by

$$\sigma = \sum_{J=0}^{\infty}\sum_{M=-J}^{+J} \exp(-E_J/kT)\exp\left(\frac{\partial_{J,M}P+\beta_{J,M}P^2}{kT}\right) \tag{B1}$$

where

$$E_J = hBcJ(J+1), \quad P = \tfrac{1}{2}\Delta\alpha E^2,$$

$$\partial_{J,M} = \lambda_1(J,M), \quad \beta_{J,M} = -\lambda_2(J,M)/hBc.$$

The terms $\lambda_1(J,M)$ and $\lambda_2(J,M)$ are given in Sec. III.

Following the procedure used by Debye,[1] σ is expanded in powers of P.[20] Defining the summations

$$\sigma_0 = \sum_{J,M} e^{-E_J/kT}, \quad \sigma_2 = \sum_{J,M} \partial_{J,M} e^{-E_J/kT},$$

$$\sigma_2' = \sum_{J,M} 2\beta_{J,M} e^{-E_J/kT}, \quad \sigma_2'' = \sum_{J,M} \partial_{J,M}^2 e^{-E_J/kT}, \tag{B2}$$

and

$$\sigma_2 = \sigma_2' + (1/kT)\sigma_2''$$

the result to terms in $P^2(E^4)$ terms is

$$\sigma = \sigma_0 + \frac{\sigma_1}{kT}P + \frac{\sigma_2}{2kT}P^2. \tag{B3}$$

Retaining only the significant components up to the second order in P, the Helmholtz free energy is

$$\phi = -kT\ln\sigma$$

$$= -kT\ln\sigma_0 - P\left(\frac{\sigma_1}{\sigma_0}\right) - \frac{P^2}{2}\left[\frac{\sigma_2}{\sigma_0} - \frac{1}{kT}\left(\frac{\sigma_2}{\sigma_0}\right)^2\right], \tag{B4}$$

where

$$\sigma_1/\sigma_0 = \tfrac{1}{3}, \quad (\sigma_1/\sigma_0)^2 = \tfrac{1}{9},$$

and in the high-temperature limit,

$$\frac{\sigma_2'}{\sigma_0} = \frac{2}{30}\frac{1}{kT},$$

$$\frac{\sigma_2''}{\sigma_0} = \frac{2}{15} + \frac{1}{15}\frac{\sum_{J=0}^{\infty}[2J+1/(2J-1)(2J+3)]e^{-E_J/kT}}{\sum_{J=0}^{\infty}(2J+1)e^{-E_J/kT}}. \tag{B5}$$

The last term in Eq. (B5) is a function of temperature and approaches zero as T goes to infinity. A numerical calculation shows that at $hBc/kT = 5\times10^{-4}$ (CS_2 at room temperature) the entire term is approximately 10^{-5}. The first term in Eq. (B4) corresponds to the unperturbed potential energy of the molecules. The second term

$$\langle \Delta W_1 \rangle = -\tfrac{1}{3}(\tfrac{1}{2}\Delta\alpha E^2) \tag{B6}$$

contributes to the electric-field-independent dielectric constant. The last set of terms gives

$$\langle \Delta W_2 \rangle = -\frac{2}{45}\frac{1}{kT}\left(\frac{\Delta\alpha}{2}E^2\right)^2, \tag{B7}$$

which implies that the nonlinear index-of-refraction coefficient n_2 is

$$\eta_2 = 2\pi N\left(\frac{2}{45}\right)\left(\frac{(\Delta\alpha)^2}{kTn_0}\right), \tag{B8}$$

where N is the number of molecules per unit volume. This is exactly the classic result.[3]

It is interesting to observe that whereas the classical partition function contains only the term $\frac{1}{2}(\Delta\alpha)E^2$; the quartic Stark shift, an energy term proportional to E^4 is necessary to evaluate n_2 quantum mechanically.

---

*NRC Postdoctoral Fellow from December 1971 to January 1973. Present address: Box 607 Havemeyer Hall, Chemistry Department, Columbia University, New York, N. Y. 10027.

†Work supported by Joint Services Electronics Program Contract USAF-F44620-71-C-0087 and NASA Grant NGR-05-003-559.

‡Work partially supported by a grant from the National Science Foundation; Alfred P. Sloan Fellow.

[1] P. Debye, *Polar Molecules* (Dover, New York, 1945).

[2]A. D. Buckingham and R. L. Disch, Proc. R. Soc. A 237, 275 (1963).
[3]N. Bloembergen and P. Lallemand, Phys. Rev. Lett. 16, 81 (1966).
[4]C. H. Lin, J. P. Heritage, and T. K. Gustafson, Appl. Phys. Lett. 19, 397 (1971).
[5]*Handbook of Mathematical Functions*, edited by M. Abramowitz and I. A. Segan (Dover, New York, 1965), p. 754.
[6]C. H. Townes and A. L. Schawlow, *Microwave Spectroscopy* (McGraw-Hill, New York, 1966).
[7]M. E. Mack, R. L. Carman, J. Reintjes, and N. Bloembergen, Appl. Phys. Lett. 16, 209 (1970).
[8]T. E. Stern, Proc. R. Soc. Lond., A 130, 551 (1931).
[9]R. F. Curl, Jr., H. P. Hopkins, Jr., and K. S. Pitzer, J. Chem. Phys. 48, 4064 (1968).
[10]L. Pauling, Phys. Rev. 36, 430 (1930).
[11]G. Herzberg, *Spectra of Diatomic Molecules* (Van Nostrand, New York, 1950).
[12]The analysis of this section, which has been confined to linearly polarized optical fields, can be easily adapted to circularly polarized fields. The ith-order coefficient of the refractive-index change induced by the latter denoted by n_i^c, is related to n_i by the simple relationship: $n_i^c = (-\frac{1}{2})^{i/2+1} n_i$.
[13]L. D. Landau and E. M. Lifshitz, *Statistical Physics* (Addison-Wesley, Reading, Mass., 1969).
[14]P. C. Cross and R. M. Hainer, J. Chem. Phys. 12, 210 (1944).
[15]J. H. Van Vleck, *Theory of Electric and Magnetic Susceptibility* (Oxford U. P., London, 1932).
[16]J. O. Hershfelder, C. F. Curties, and R. B. Bird, *Molecular Theory of Gases and Liquids* (Wiley, New York, 1954).
[17]G. Herzberg, *Electronic Spectra and Electronic Structure of Polyatomic Molecules* (Van Nostrand, New York, 1966).
[18]The observation of the optically induced retractive index and the first delayed burst in refractive index in CS_2 vapor has recently been reported. J. P. Heritage, C. H. Lin, and T. K. Gustafson, *Digest of Technical Papers*, Eighth International Quantum Electronics Conference, IEEE J. Quantum Electron. QE-10, 724 (1974).
[19]M. A. Duguay and J. W. Hansen, Appl. Phys. Lett. 15, 192 (1969).
[20]There is an error in Eq. (111) of Ref. 1. A factor of kT should multiply the last term on the right-hand side. The equations following should change accordingly.